Since January 2020 Elsevier has created a COVID-19 resource centre with free information in English and Mandarin on the novel coronavirus COVID-19. The COVID-19 resource centre is hosted on Elsevier Connect, the company's public news and information website.

Computers in Biology and Medicine 146 (2022) 105502

Contents lists available at ScienceDirect

Computers in Biology and Medicine

journal homepage: www.elsevier.com/locate/compbiomed

Unveiling the nature's fruit basket to computationally identify *Citrus sinensis* csi-mir169–3p as a probable plant miRNA against Reference and Omicron SARS-CoV-2 genome

Naman Mangukia [a,d], Priyashi Rao [b], Kamlesh Patel [e], Himanshu Pandya [a], Rakesh M. Rawal [b,c,*]

[a] Department of Botany, Bioinformatics and Climate Change Impacts Management, School of Sciences, Gujarat University, Ahmedabad, 380009, Gujarat, India
[b] Department of Biochemistry and Forensic Science, University School of Sciences, Gujarat University, Ahmedabad, 380009, Gujarat, India
[c] Department of Life Science, University School of Sciences, Gujarat University, Ahmedabad, 380009, Gujarat, India
[d] BioInnovations, Bhayander (West), Mumbai, 401101, Maharashtra, India
[e] Advait Theragnostics, GUSEC, Gujarat University, Ahmedabad, 380009, Gujarat, India

ARTICLE INFO

Keywords:
Dietary plant miRNAs
SARS-CoV-2
miRNA-target interaction
Conserved 3′UTR
Omicron (B.1.1.529) variant
Computational genomics

ABSTRACT

The fundamental role of microRNAs (miRNAs) has long been associated with regulation of gene expression during transcription and post transcription of mRNA's 3′UTR by the RNA interference mechanism. Also, the process of how miRNAs tend to induce mRNA degradation has been predominantly studied in many infectious diseases. In this article, we would like to discuss the interaction of dietary plant miRNAs derived from fresh fruits against the viral genome of the causative agent of COVID-19, specifically targeting the 3′UTR of SARS-CoV-2 (Severe acute respiratory syndrome coronavirus 2) genome. Expanding the analysis, we have also identified plant miRNAs that interact against the Omicron (B.1.1.529) variant of SARS-CoV-2 across 37 countries/territories throughout the world. This cross-species virus-plant interaction led us to identify the alignment of dietary plant miRNAs found in fruits like *Citrus sinensis* (Orange), *Prunus persica* (Peaches), *Vitis vinifera* (Grapes) and *Malus domestica* (Apple) onto the viral genomes. In particular, the interaction of *C. sinensis* miRNA - csi-miR169–3p and SARS-CoV-2 is noteworthy, as the targeted 3′UTR region "CTGCCT" is found conserved amongst all curated 772 Omicron variants across the globe. Hence this site "CTGCCT" and miRNA csi-miR169–3p may become promising therapeutic candidates to induce viral genome silencing. Thereby, this study reveals the mechanistic way of how fruits tend to enact a fight against viruses like SARS-CoV-2 and aid in maintaining a strong immune system of an individual.

1. Introduction

The world has frequently faced unexpected epidemics caused by viral infections which continue to be a threat for the human population taking its tolls on incalculable lives. The recent events along with many past epidemics express how viral diseases spread rapidly. Throughout the millennium, our planet has witnessed thousands of such outbreaks from the "black death" bubonic plague of the 14th century to the great smallpox pandemic, the yellow fever infection of the 16th century, the 18th century dengue virus fever, followed by the epidemic of Human Immunodeficiency Virus (HIV), and the recent SARS-CoV-2 pandemic [1].

The coronavirus infection of 2019 emerged as an outbreak in late 2019 and shuddered the entire world. The infection is caused by the Severe Acute Respiratory Syndrome Coronavirus-2 (SARS-CoV-2) and the surge of infection related morbidities was so extreme that the World Health Organization (WHO) had to declare COVID-19 as a global pandemic in March of year 2020 [2]. As of 9th March 2022, more than 446 million cases of COVID-19 infection were reported, taking toll on 6 million lives worldwide as per WHO statistics [3]. The common symptoms being fever or chills, cough, headache, shortness of breath, muscle or body aches, altered sense of taste or smell, sore throat, congestion, nausea or vomiting, runny nose and even diarrhoea [4].

The starkest emergence is the SARS-CoV-2 related secondary infections of *Aspergillus or Rhizopus* related Mucormycosis. Also termed as COVID-19 Associated Mucormycosis (CAM) is known to affect those that

* Corresponding author. Department of Life science, University School of Sciences, Gujarat University, Ahmedabad, 380009, Gujarat, India.
E-mail addresses: namanmangukia@gujaratuniversity.ac.in (N. Mangukia), priyashi.rao@gujaratuniversity.ac.in (P. Rao), kamlesh.patel@advaitdx.com (K. Patel), hapandya@gujaratuniversity.ac.in (H. Pandya), rakeshrawal@gujaratuniversity.ac.in (R.M. Rawal).

https://doi.org/10.1016/j.compbiomed.2022.105502
Received 12 January 2022; Received in revised form 28 March 2022; Accepted 4 April 2022
Available online 8 April 2022

have a weakened immune system probably due to underlying health comorbidities like diabetes, organ transplantation, or undergoing chemotherapy [5]. The conditions worsened with the onset of the second wave of COVID-19 and the virus continued to evolve showcasing a similar symptom pattern and giving rise to various variants of interests (VOI). Later, on November 26, 2021 an identified mutant strain, known as B.1.1.529, was classified as a variant of concern (VOC) and was named Omicron on the advice of WHO's Technical Advisory Group on Virus Evolution (TAG-VE) [6]. On the current WHO list of VOCs, Omicron joins Alpha, Beta, Gamma and Delta variants of SARS-CoV-2. Omicron seems to have a high number of mutations in its spike protein, which is the primordial target of the host immune response and is also the vaccine target. These mutations are likely to impair the antibodies' capacity to identify the virus and inhibit the viral infection [7]. Apparently, the sharp rise in cases of the Omicron variant in South Africa's Gauteng province is a witness to that. The alarm was set off by the identification of a genome-sequencing data of B.1.1.529 from Botswana. This Omicron variant had more than 30 changes on the SARS-CoV-2 spike protein. Albeit many of such mutations were identified in other VOCs as well, like Delta and Alpha variant however, transmission of the Omicron variant prompts scientists to study how much this new variant could jeopardise the existing vaccinated population [8]. This serves as the bleak reminder that this war is not yet concluded.

As prevention is always a key, all these events advocate that a well-balanced nutritious diet is inevitable for a healthy life. The synergy between balanced diet and nutrition in strengthening the immune system to fight diseases has long been recognized. Nearly 2500 years ago Hippocrates said, "Let food be thy medicine and medicine be thy food", suggesting that an individual's health status is influenced by both food consumption and disease occurrence [9]. Specific foods or dietary combinations have been known to strengthen the immune system. It's critical to have enough selenium, zinc, iron, and vitamins like A, B 12, B6, C, and E to keep one's immune system healthy [10]. Consequently, dietary habits are important elements of gut microbial composition and, as a result, can influence immune response state of the body [11]. Considering that plants are the primary source of food to many, it is critical to recognise and assess the potential influence of ingested plant miRNAs on host gene expression.

miRNAs belong to a class of single-stranded noncoding RNA of approximately 18–23 nucleotides. miRNAs are an integral part of a eukaryotic cell which are responsible for playing a significant part in regulating the gene expression at the post transcriptional level [12]. Most miRNAs are synthesised from DNA sequences as primary miRNAs and then precursor miRNAs and ultimately form mature miRNAs. To disrupt the process of protein translation, miRNAs engage with 3′UTR of target mRNAs to induce translational repression or mRNA destruction to eventually cause miRNA mediated gene silencing [13]. A plant-based diet allows us to absorb the genetic material and nucleic acids that include a considerable amount of plant miRNA. These dietary miRNAs, then enter our body owing a potential to interact with our body's existing nucleic acids. The small miRNAs in fruit when released into the human body, are found to be stable and functional as acidification did not significantly affect the yield and quality of miRNAs. Also, food-derived exogenous plant MIR168a can pass through the mouse gastrointestinal (GI) track and enter the circulation. Evidence suggests that the levels of food derived plant miRNAs in various serum samples were about one-tenth of that of endogenous miR-16 [14] and when plant RNAs were added directly to food pellets, plant miRNA fragments were also detected in the faeces, GI tract, circulation and reach organs [15–17]. There are innumerable *in vitro* evidences which describes the mechanism of action of dietary miRNA and discuss how dietary miRNA are resistant to enzymatic digestion and remain functional. The ingested plant miRNAs remain unaffected by stomach acidification and transit through the gastrointestinal system, enter the bloodstream to reach tissues, for regulating a particular gene expression in mammals and are found to be excreted in urine [14,18]. The proactive influence of plant miRNA is not just reduced with being an anti-viral, but it's also proven to initiate anti-inflammatory, anti-cancer as well as immuno-regulatory affects upon regular consumption of the plant/herb decoction [19].

There is evidence of a plant derived miRNA namely, miRNA2911 obtained from honeysuckle (*Lonicera* sp.*)* decoction having anti-viral activity against the common cold influenza virus, H1N1, H5N1 and H7N9. Also, miRNA2911 is considered to be the first active plant miRNA identified from Traditional Chinese Medicine (TCM) to induce suppression by aligning to the PB2 and NS1 gene sequences of H1N1 encoded influenza virus [20]. Recently, the same miRNA2911 derived from the honeysuckle decoction was found to align at about 28 binding sites on the SARS-CoV-2 reference genome. *In vitro* exosomal MIR2911 depicted 93% of suppression of viral replication upon interacting with its genome. Likewise, it was observed in the clinical study with SARS-CoV-2 infected patients who were orally administered the honeysuckle decoction. Besides, periodic consumption of the honeysuckle decoction and adequate assimilation of MIR2911 in COVID-19 patients aided in accelerating the course of treatment and prevented further escalation of the infection in both male and female patients [21]. Plant miRNAs like miR156 and miR168 from strawberry, miR168 from rice, and miR874 from cabbage, revealed that the miRNAs could modify the ability of dendritic cells to respond to inflammatory agents by limiting T-cell proliferation, therefore reduce inflammation herein acting as immunomodulatory agents [22]. With the immense spread of this disease, many such studies have been conducted involving cross-kingdom plant-virus relationship. A recent study undertaken by our research group pinpointed a conserved 'GGAAGAG' site on the 3′UTR of the worldwide submitted SARS-CoV-2 whole genomes. A total of five plant miRNAs from three medicinal plants *Ocimum tenuiflorum*, *Piper nigrum* and *Zingiber officinale* were obtained having potential to align with the SARS-CoV-2 3′ UTR region. From a family of plant miRNAs, mir477 and miR2673 were identified to bind and regulate the expression of SARS-CoV-2 viral mRNA using *in-silico* approach [23].

This research work describes how plant derived miRNAs, mainly the ones that can be directly consumed as raw food and could perhaps be a part of cross kingdom interactions with the potency to curb the virion of SARS-CoV-2 and its most recent Omicron variant. This work also provides an unexplored insight into a plausible immunomodulatory action of a nutritious fruit like *Citrus sinensis*.

2. Material and methods

2.1. SARS-CoV-2 genome retrieval

National Centre for Biotechnology Information (NCBI) (https://www.ncbi.nlm.nih.gov/) is a repository of biological information and online resources. GenBank is one of the database of NCBI consisting the information and retrieval system for nucleic acid sequences [24]. The reference genome sequence of SARS-CoV-2 was downloaded from NCBI (GenBank accession: NC_045512.2). The Untranslated regions (UTR) and Coding Sequence (CDS) regions of the sequence are described in Fig. 1A along with the entire study briefings in section B. The sequence of this reference genome consists mostly of three regions: the 5′UTR (1–265: 265 bases), the CDS (266–29674: 29,409 bases) lead by a flanking 3′UTR (29675–29903). The SARS-CoV-2 genome has 14 open reading frames (ORFs), with the first ORF accounting for roughly 68% of the genome (coding 16 non-structural proteins (nsps)), and the remaining ORFs coding for accessory and structural proteins.

2.2. Plant mature miRNA sequences

miRBase (https://www.mirbase.org/) [25] established in 2002, is one such miRNA database responsible for handling the nomenclature of miRNA and updating the novel identified entries in the repository regularly. Broadly the miRBase database comprises of sequences,

Fig. 1. A. A representation of SARS-CoV-2 reference genome (Genbank, NC_045512.2): 5′UTR, CDS and 3′UTR regions with the scale of 1000 bases (1k) unit. The 3′UTR region is explored with its bases. B. Study workflow: depicts the major steps undertaken in this study.

research articles, sequencing data along with genomic location of miRNAs. Each individual entry in the miRBase provides information of a predicted hairpin portion of the miRNA transcript (called as 'miR') in the database. Both hairpin and mature sequences are available for searching, browsing, and entries can also be retrieved by name, keyword, references, and annotations.

The current version (v22.1) of miRBase consists of 38,589 stem-loop precursor and 48,860 mature sequences of 271 organisms divided mainly in 6 categories namely, as *Alveolata*, *Chromalveolata, Metazoa, Mycetozoa, Viridiplantae* and *Viruses*. As plant miRNAs is the primary focus for this study, the *Viridiplantae* eukaryotic clade was explored under the 'browse' tab in miRBase. Furthermore, the *Viridiplantae* clade is divided in 4 subcategories – *Chlorophyta, Coniferophyta, Embryophyta* and *Magnoliophyta,* out of which *Magnoliophyta* consists of highest 75 organisms. A total of 10,414 plant mature miRNA sequences of 82 organisms were downloaded individually from the *Viridiplantae* clade.

2.3. Targeting plant miRNAs on SARS-CoV-2 3′UTR

The miRanda algorithm [26] is utilized for the detection of potential microRNA target sites in genomic sequences. To do that, it performs a 3-phase process to identify the target site using its sequence information. Phase-1 initiates with a possibility of complementary binding between query miRNA and target mRNA sequences. This phase uses local alignment Smith-Waterman algorithm [27] with complementary match. Phase-2 is the free energy calculation for physical interaction of miRNA and mRNA energetics. To achieve this, the algorithm utilizes RNA folding package by Wuchty and co-workers [28]. Phase-3 is processed with the knowledge-based filter having core concept of evolutionary conservation. All 10,414 plant mature miRNA sequences were complementary searched against 3′UTR of SARS-CoV-2 genome through miRanda algorithm (standalone version: 3.3a). The obtained hits were primary filtered using two parameter thresholds: i) minimum energy of $\Delta G \leq -14$ kcal/mol of the miRNA: 3′ UTR duplex and ii) hybridization alignment score ≥ 80. These primary hits were processed further under the criteria of 7 site types (Fig. 2) resulted in the final hits [29]. In this study, these 7 site types are broadly categorized into two types on the norms of alignment initialisation position: i) 2nd position site and ii) 3rd position site. The final hits were then selected to obtain hits in dietary 'raw eatable' plants or fruits.

2.4. Targeting plant miRNAs on Omicron variant (B.1.1.529)

The genome sequences of Omicron variant of SARS-CoV-2 were retrieved from GISAID (Global initiative on sharing all influenza data) [30] repository as of Dec-22-2022. Sequences with length<29,700 bases were removed. 3′UTR portion from each sequence was retrieved and N/n containing sequences were discarded followed by Poly-A tail region removal at the 3′ end using the *in-house* Perl scripts. The 3′UTR region of SARS-CoV-2 reference genome (NC_045512.2) was added with the

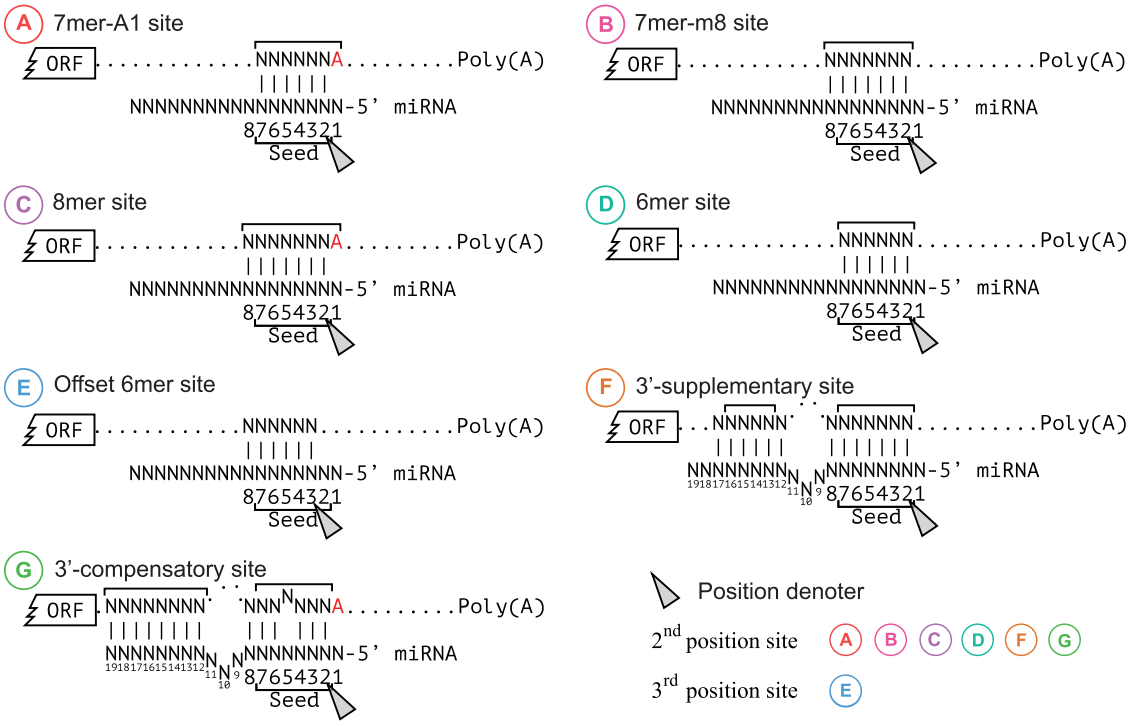

Fig. 2. Site types adapted from Bartel,2009 [29]. Each of these 7 site types are having mainly two components: mRNA (up-side, direction: 5'->3') and miRNA (down-side, direction: 3'->5'). The square bracket is used to pinpoint seed-match alignment region on mRNA and similarly used to highlight the seed region in miRNA. These site-types were further classified on the bases of alignment start position i.e., 2nd position site-types and 3rd position site types. Site-types A, B, C, D, F and G are falling in the 2nd position category while E is in 3rd position Site-type. As depicted, a triangle shape marker has been used to pinpoint the alignment start position.

finalized 3′UTR regions and processed for Multiple Sequence Alignment (MSA) using Clustal Omega (standalone version: 1.2.4) [31]. The obtained dietary 'raw eatable' fruit miRNAs as mentioned in method section 2.3 were applied on this combined result of MSA to find the conserved region amongst the 3′UTR of the Omicron variants.

2.5. Searching conserved site in other variants of SARS-CoV-2

To find the conserved site availability in other SARS-CoV-2 variants, the related information of VOC and VOI was retrieved from WHO website [6]. The respective genome sequences were downloaded using the 'Pango lineage' keyword search from NCBI as of February 8, 2022. To fetch the curated sequences of 3′UTR and the conserved site search amongst them, all the retrieved variant genomes were filtered with the same filtering criteria as mentioned in the previous section.

2.6. Molecular dynamics (MD) simulation for 3′UTR-miRNA complex

MD simulation was performed for the interaction of SARS-CoV-2 3′UTR-miRNA complex with lowest minimum energy. The DNA sequence alignment for 3′UTR was modified manually so that it corresponded to the nucleotide sequence of RNA. RNAfold web server [32] (http://rna.tbi.univie.ac.at/cgi-bin/RNAWebSuite/RNAfold.cgi) was used to predict the secondary structure for SARS-CoV-2 3′UTR (5′-CAAUGCUAGGGAGAGCUGCCUA-3′) and csi-miR169–3p (3′-GAAUCGGUUCCUCUUGACGGAC-5′). The dot-bracket format of the secondary structure was used as an input file to model the RNA 3D structure using RNAComposer [33,34] (https://rnacomposer.cs.put.poznan.pl/), a fully automated online RNA 3D structure modelling server. The obtained PDB files for the 3D structure of 3′UTR and csi-miR169–3p interaction was assembled using the 'Build Structure' wizard of UCSF Chimera 1.11 [35] (https://www.cgl.ucsf.edu/chimera/). Optimisation for MD simulation of the nucleotide complex was done by assigning Gasteiger charges, hydrogen bonds, energy minimization at 500 steepest descents with a step size of 0.04 Å at an update interval of 10 in 'Dock Prep tool' of UCSF Chimera 1.11. To carry out the simulation, 3′UTR-miRNA complex was imported to GROMACS [36–38] (http://www.gromacs.org/), topology was created using 'Gromacs utilities' with AMBER94 force field. Water model was set to Simple Point Charge (SPC). Unit cell box of dodecahedron shape over the 3′UTR-miRNA complex was defined under periodic boundary conditions with 1.0 nm buffer distance from the periphery of the 3′UTR-miRNA complex and then filled with water molecules. Then, the Unit box containing a system of 3′UTR-miRNA complex and water molecules was neutralized by Cl− or Na + counter ions. Steepest descent energy minimization of this system was performed, followed by equilibration and MD simulation run with NVT (constant number of particles, volume, and temperature) conditions for 20 ns at 295 K. The LINCS (Linear Constraint Solver) technique was used to restrict all of the covalent bonds [39]. The Particle Mesh Ewald (PME) approach was used to address the electrostatic interactions and for and the cut-off radii were chosen to be 10.0 Å for Coulomb interactions and 14.0 Å for van der Waals interactions. MD trajectories were assessed after MD simulation for Root-Mean-Square Deviation (RMSD), Root-Mean-Square Fluctuation (RMSF), radius of gyration (Rg), and the number of H-bonds formed inside the UTR-miRNA complex, and the 'XMgrace tool' [40] was used to generate the graphs.

3. Results

3.1. Identification of plant miRNA target sites within SARS-CoV-2 3′UTR genomic region

The SARS-CoV-2 is a positive single stranded RNA virus comprising

of 29903 bases long genome. Its genomic structure comprises well defined UTR (position: 1–265[5′UTR], 29675–29903[3′UTR]) and CDS (position: 266–29674) segments (NCBI Reference Sequence: NC_045512.2). The majority region of genome, CDS contains 10 ORFs with Structural (mainly ORF1a and ORF1b) and Non-structural (S, E, M and N) protein coding genes by spanning 98.348% of the genome sequence [41], while only 1.652% region is covered by UTR. MicroRNAs are the class of non-coding RNAs having great binding affinity towards the targeted mRNA's 3′UTR region [42].

All 10,414 plant miRNAs were aligned using miRanda algorithm against the 3′UTR of SARS-CoV-2 genome, which resulted in 220 target hits. After applying primary filtration with $\Delta G \leq -14.00$ and score$\geq$80 [26], a total of 148 hits remained. A further stringent filtration was applied as per the site types [29] resulted in a total of 111 miRNAs belonging to genera of 34 plants that were aligned with the 3′UTR of SARS-CoV-2 genome. Out of the total of 111 plant miRNAs, *Medicago truncatula* stood at top with 13 hits followed by *Citrus sinensis* (12 hits), *Oryza sativa* (9 hits), *Manihot esculenta* (9 hits), *Physcomitrella patens* (6 hits), *Glycine* max (6 hits), *Zea mays* (5 hits), *Populus trichocarpa* (5 hits), *Brachypodium distachyon* (5 hits), *Aquilegia caerulea* (5 hits), *Nicotiana tabacum* (4 hits), *Solanum tuberosum* (3 hits), *Picea abies* (3 hits), *Malus domestica* (2 hits), *Lotus japonicus* (2 hits), *Hordeum vulgare* (2 hits), *Gossypium raimondii* (2 hits), *Eugenia uniflora* (2 hits), *Vitis vinifera* (1 hit), *Vriesea carinata* (1 hit), *Saccharum* sp. (1 hit), *Solanum lycopersicum* (1 hit), *Sorghum bicolor* (1 hit), *Rehmannia glutinosa* (1 hit), *Phaseolus vulgaris* (1 hit), *Pinus taeda* (1 hit), *Prunus persica* (1 hit), *Hevea*

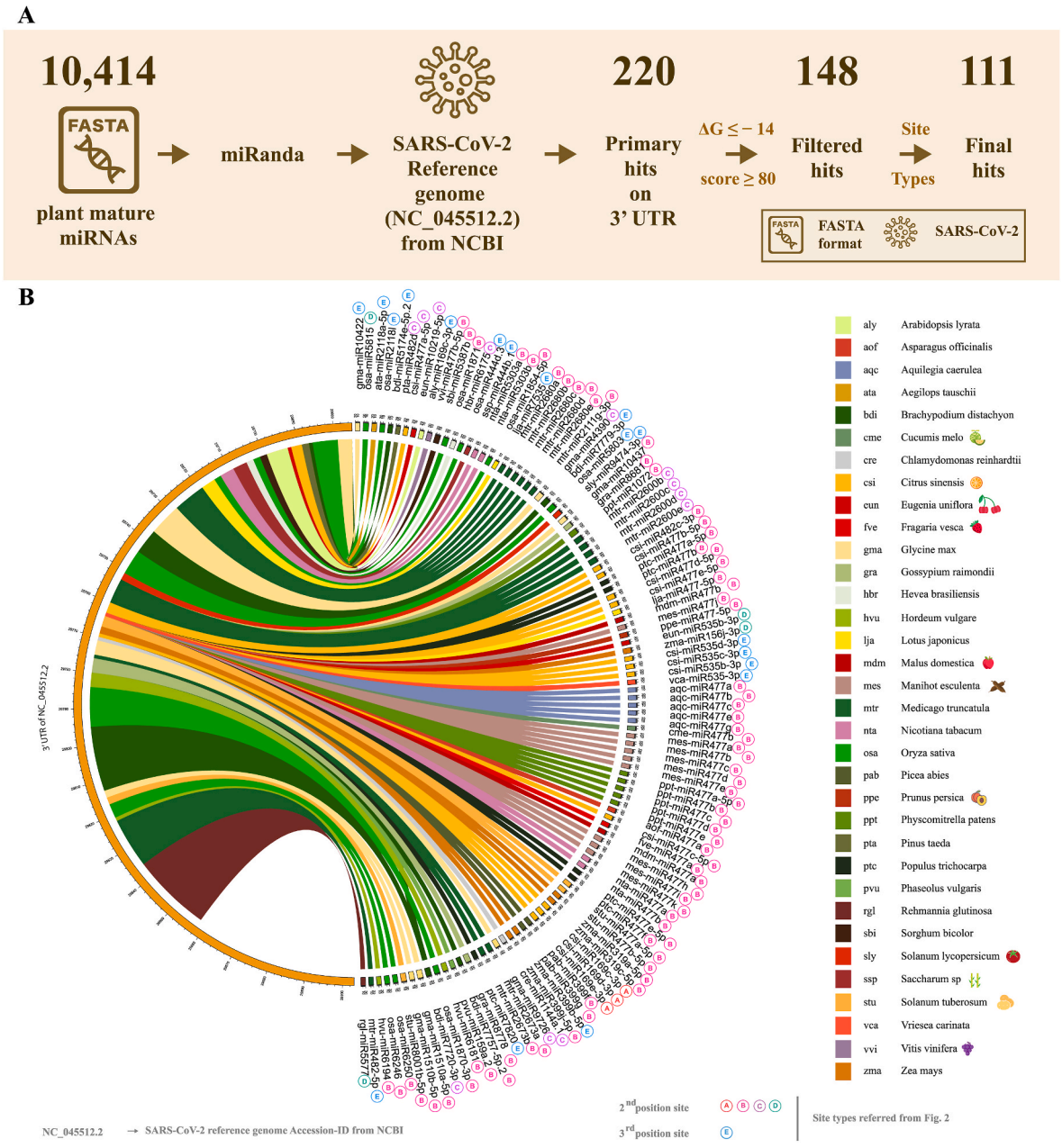

Fig. 3. **A.** This section highlights the stepwise workflow of the obtained 111 hits. **B.** Circos representation of 111 interactions between plant miRNAs and their targets on the 3′UTR region of SARS-CoV-2 reference genome: The main ideogram is divided into two parts: i) left side half portion is 3′UTR region of SARS-CoV-2 reference genome (NC_045512.2), where its length is displayed on 1-base scale. The right-side half portion is of 111 hits from 34 plant miRNAs: Starting with the length scale of 1-base followed by the miRNA names. Respective site-types are mentioned after the miRNA names as referred from Fig. 2. The connection between miRNAs and their targets is displayed by ribbons, where the color of each ribbon is organism-wise assigned as given in right side panel. Right side panel is displayed to show the utilized features of 34 plant organisms with 3 columns: i) Organism-wise color palette, ii) miRBase 3-letter prefix and iii) Organism names.

brasiliensis (1 hit), *Fragaria vesca* (1 hit), *Chlamydomonas reinhardtii* (1 hit), *Cucumis melo* (1 hit), *Aegilops tauschii* (1 hit), *Asparagus officinalis* (1 hit) and *Arabidopsis lyrata* (1 hit). The procedure and these 111 interactions are depicted in Fig. 3.

3.2. Edible plant miRNAs' targets on SARS-CoV-2 3′UTR

The 111 filtered plant miRNA targets were screened on the criteria of 'raw-eatable plants'. This was done to ensure that the genetic component remains stable and intact while consuming the plant and not get degraded while cooking or heating; nonetheless there are reports which describe that mature plant miRNAs like miR168a, obtained from edible-food sources can often be detected in cooked food and even remain intact and active after enzymatic digestion in the gastrointestinal tract [14]. However, just to steer clear of any ambiguity, we have taken into consideration only plant miRNA hits from 'raw-eatable' plants. In totality, out of 111 hits, only 21 of the plant miRNAs were identified under the category of 'raw-eatable' plants. These were able to target and get complementarily aligned to the SARS-CoV-2 3′UTR as well. These 3′UTR targeting plant miRNAs were found to be from 8 edible fruits, namely *Citrus sinensis* (12 hits), *Eugenia uniflora* (2 hits), *Malus domestica* (2 hits), *Prunus persica* (1 hit), *Vitis vinifera* (1 hit), *Cucumis melo* (1 hit), *Fragaria vesca* (1 hit) and *Saccharum* sp. (1 hit). Further, to mention these 21 miRNAs are: cme-miR477b, csi-miR169c-3p, csi-miR169d-3p, csi--miR169e-3p, csi-miR477a-5p, csi-miR477b-5p, csi-miR477c-5p, csi--miR477d-5p, csi-miR477e-5p, csi-miR482c-3p, csi-miR535b-3p, csi-miR535c-3p, csi-miR535d-3p, eun-miR10219–5p, eun-miR535b-3p, fve-miR477a, mdm-miR477a, mdm-miR477b, ppe-miR477–5p, vvi-miR477b-5p and ssp-miR444b.1. The interaction between fruit miRNAs and SARS-CoV-2 3′UTR reference has been depicted in Fig. 4

A

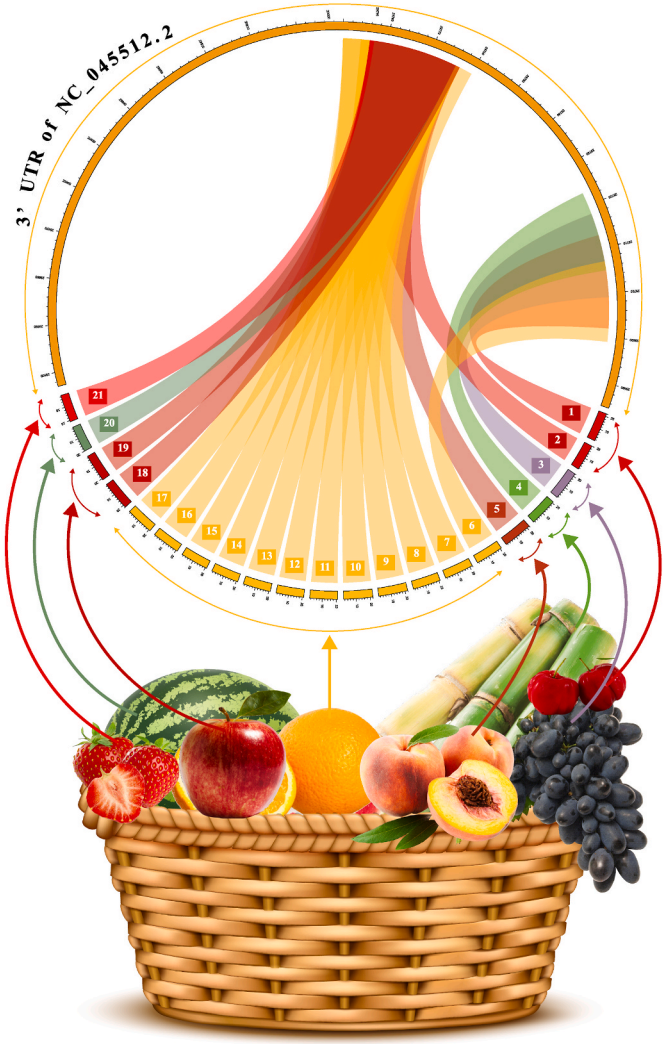

B

miRBase prefix	Scientific Name	Common Name	Number of Fruit miRNAs targeting SARS-CoV-2 3'UTR	Respective serial numbers of Fruit miRNAs
csi	Citrus sinensis	Orange	12	6 7 8 9 10 11 12 13 14 15 16 17
cme	*Cucumis melo*	Watermelon	1	20
eun	*Eugenia uniflora*	Surinam Cherry	2	1 2
fve	*Fragaria vesca*	Wild Strawberry	1	21
mdo	*Malus domestica*	Apple	2	18 19
ppe	*Prunus persica*	Peach	1	5
ssp	*Saccharum sp.*	Sugarcane	1	4
vvi	*Vitis vinifera*	Grapes	1	3

Fig. 4. Edible fruit miRNAs and their targets on 3′UTR of SARS-CoV-2 reference genome: **A.** Nature's fruit-basket Circos view: This section depicts the 8 edible fruit's 21 miRNAs and their respective targets on 3′UTR of SARS-CoV-2 reference genome as lower and upper layer respectively. The length scale is set as 1-base unit. Respective portion of fruit miRNAs are pinpointed by the fruits depicted in the fruit-basket. Fruit miRNAs and their targets are shown by respective color ribbons, where the color assignment has been as per the palette given in Fig. 3. B. Each ribbon is tagged by a serial number in square box belonging to the specific fruit miRNAs as mentioned in section B. **B.** Tabular view having five columns information of 8 edible fruit miRNAs: i) miRBase 3 letter prefix, ii) Scientific name, iii) Common name, iv) 3′UTR interacting fruit-miRNA counts and v) Respective serial numbers of fruit miRNAs.

and related miRanda result statistics is described in Fig. 5.

As depicted in Fig. 4, *Citrus sinensis* (Orange) is having maximum 12 interacting miRNAs against the 3′UTR of SARS-CoV-2 followed by *Eugenia uniflora* (Surinam Cherry) and *Malus domestica* (Apple) with 2 miRNAs.

As shown in Fig. 5, all miRNAs are having experimental evidence except the 2 miRNAs ssp-miR444b.1 and cme-miR477b. The score values are ranging from 140 to 153 and the free energy (ΔG) values are ranging between −26.68 and −14.09 out of which csi-miR169c-3p, csi-miR169d-3p and csi-miR169e-3p consist lowest free energy i.e. −26.68

A

Sr. No.	miRNA	Evidence from miRBase	miRanda results								
			Score	Energy△G (Kcal/Mol)	Alignment				Length	Identity in %	
					Query		Target			Target	Query
					Start	End	Start	End			
1	eun-miR10219-5p	Illumina	141.00	-14.09	2	10	29692	29713	8	87.50	100.00
2	eun-miR535b-3p	Illumina	140.00	-19.68	2	19	29763	29785	20	70.00	80.00
3	vvi-miR477b-5p	Illumina	153.00	-16.97	2	21	29699	29718	19	68.42	78.95
4	ssp-miR444b.1	Not Experimental	144.00	-17.64	3	20	29705	29723	17	82.35	82.35
5	ppe-miR477-5p	Illumina	147.00	-17.82	2	20	29763	29784	18	66.67	66.67
6	csi-miR535d-3p	Illumina	145.00	-19.64	3	20	29763	29786	20	80.00	80.00
7	csi-miR535c-3p	Illumina	145.00	-19.64	3	20	29763	29786	20	80.00	80.00
8	csi-miR535b-3p	Illumina	145.00	-19.64	3	20	29763	29786	20	80.00	80.00
9	csi-miR477a-5p	Illumina	143.00	-14.59	2	19	29689	29707	17	70.59	70.59
10	csi-miR482c-3p	Illumina	141.00	-14.54	2	10	29760	29781	8	87.50	100.00
11	csi-miR477b-5p	Illumina	140.00	-18.69	2	9	29763	29783	7	100.00	100.00
12	csi-miR477d-5p	Illumina	145.00	-16.97	2	10	29763	29784	8	100.00	100.00
13	csi-miR477e-5p	Illumina	145.00	-16.97	2	10	29763	29784	8	100.00	100.00
14	csi-miR477c-5p	Illumina	145.00	-19.91	2	10	29764	29784	8	100.00	100.00
15	csi-miR169c-3p	Illumina	152.00	-26.68	2	18	29769	29790	17	76.47	94.12
16	csi-miR169d-3p	Illumina	152.00	-26.68	2	18	29769	29790	17	76.47	94.12
17	csi-miR169e-3p	Illumina	152.00	-26.68	2	18	29769	29790	17	76.47	94.12
18	mdm-miR477b	miRNAseq	145.00	-19.01	2	10	29763	29784	8	100.00	100.00
19	mdm-miR477a	miRNAseq	145.00	-16.36	2	10	29764	29784	8	100.00	100.00
20	cme-miR477b	Not Experimental	142.00	-18.30	2	19	29764	29783	17	64.71	64.71
21	fve-miR477a	Illumina	145.00	-16.48	2	10	29764	29784	8	100.00	100.00

B

Fig. 5. A. The section shows four column information of 21 fruit miRNAs: i) Serial number, ii) Name of the miRNA, iii) Evidence of the miRNA from miRBase and iv) miRanda results. The miRanda results column is divided into the sub-columns to show the detailed statistics. **B.** Alignment interaction between each 21 edible fruit miRNAs and respective 3′UTR region of SARS-CoV-2 reference genome along with the site type information.

kcal/mol with the second maximum score value of 152 reflect their strong binding affinity towards the 3′UTR targets compare to the other miRNAs.

3.3. Edible plant miRNA targets on Omicron variant of SARS-CoV-2

To check whether these 8 fruit miRNAs can target the recent SARS-CoV-2 variant of concern Omicron (B.1.1.529), we retrieved a total of 20,455 SARS-CoV-2 genomic records of Omicron as of Dec-22-2021 in FASTA format from GISAID repository. As identified, mutations in the Omicron variant are seen in a variety of SARS-CoV-2 proteins, including Spike protein, NSP3, membrane protein, NSP4, NSP5, envelope protein, NSP6, NSP12, NSP14, and nucleocapsid protein. With expected or unknown genetic modifications of what this variant harbour, it surely does impact features like transmissibility of the infection, illness severity, and immune escape mechanism. For all these retrieved SARS-CoV-2 variant sequences, the 3′UTR region was extracted, followed by the filtering process of short length sequences and sequences having multiple N's. This was performed using *in-house* Perl scripts. Finally, 770 sequences of Omicron variant of SARS-CoV-2 3′UTR were obtained belonging to 37 various countries/territories globally. The methodology steps and relative regions with their counts of the obtained 3′UTRs are mentioned in Section A and B of Fig. 6 respectively. These all 770 filtered sequences were processed for MSA using Clustal Omega, along with the SARS-CoV-2 reference genome 3′UTR (NC_045512.2) to find the sequence conservation amongst them. Fig. 6C describes the base conservation between the 3′UTR region of reference and Omicron variants of SARS-CoV-2 genomes.

Out of the 20,455 sequences of Omicron variants, only 770 3′UTR records were retrieved and the rest were discarded due to the short length and presence of N/n residues. This Omicron sequence data mix was with South Africa at the top with 210 counts followed by USA with 180 counts and the remaining from other regions. Apart from the Poly-A tail residues, a total of 117 (~60%) bases are still unchanged compared to the first reported reference genome of SARS-CoV-2 [43] while observing the conservation analysis depicted in Section C of Fig. 6. A total of 21 fruit miRNAs targeted 3′UTR region is broadly divided into the 2 clusters: Cluster-1 consists of 4 miRNAs (Serial number – 9, 1, 3 and 4) namely: csi-miR477a-5p, eun-miR10219–5p, vvi-miR477b-5p and ssp-miR444b.1, spanning the 22 bases targeted region – "AGGGAGGACTTGAAAGAGCCAC" (29,700–29721). Except the base 'G' (position: 29706), all residues of this Cluster1 3′UTR region are conserved across the Omicron variants. Cluster-2 harbouring rest all 17 fruit miRNAs' targeting 3′UTR region with 16 bases - "CTAGGGAGAGCTGCCT" (29774–29789). Compared to the Cluster-1, Cluster-2 is smaller in length, but the major gathering of the fruit miRNAs has been found on this locus. Cluster-2 comprises of 2 non-conserved bases 'GG' (position: 29778–29779). Another remarkable observation was that, out of 21 fruit miRNAs, 11 are of miR477 family, which shows the potential of this family against the SARS-CoV-2 virus genome.

The conserved site "CTGCCT" was also identified in other VOC's (alpha, beta, gamma, delta and lambda) and VOI (MU variant) as shown in Fig. 7, which accounts for the variant lineage and the count of conserved site "CTGCCT" sequence in percentage for the evolving strains of novel SARS-CoV-2.

3.4. MD simulation assessment for 3' UTR and csi-miR169–3p duplex

The lowest binding energy conformer of SARS-CoV-2 3′ UTR and csi-miR169–3p RNA duplex was −26.68 kcal/mol, subjected to 20 ns MD simulation, and the trajectories were computed in graphical form (Fig. 8) as RMSD, RMSF, Radius of gyration and number of hydrogen bond interactions. The RMSD is a crucial parameter to analyse the equilibration of MD trajectories. RMSD of the 3′UTR-miRNA complex atoms are plotted as a function of time to check the stability of the system throughout the 20 ns simulation. The RMSD values were calculated against the simulation time scale, 0–20 ns and the results are plotted in Fig. 8 A. The average of RMSD values of the complex of the entire MD simulation run was less than 1.0 nm and occasionally the peaked ~1.7 nm. Further, analysis of the RMSD graph indicates that all atoms were within 1.75 nm during the course of the MD simulations relatively to the initial conformation. From 0 to 2.5 ns (up to 2500 ps), the RMSD gradually increased from the value zero (origin of the graph) with time and attained the value equal to the average value of 1.0 nm suggesting the 3′UTR-miR complex to have attained the stability at ~2.5 ns. Further, the MD simulations from 2.5 ns to 10 ns the complex did not render any major alteration in the stability of the complexes as the RMSD trend in this time frame remained uniform.

The RMSF with respect to the average MD simulation conformation reflects as a means of portraying flexibility differences amongst the RND duplex complex. The high RMSF value indicates more flexibility whereas the low RMSF value indicates limited movements during simulation in relation to its average position. The RMSF of the residues are shown in Fig. 8 B. RMSF of all the atoms of the complex never exceeds 0.07 nm except atoms 650–700 which may be due to the mismatch base-pair T-G and G-U, but this mismatch didn't destabilise the RNA-RNA complex. Atoms before 650 and after 700 have been displaying a rather lower and stable trend in RMSF values.

The intra molecular hydrogen bonds between complementary base pairs of two antiparallel strands of 3′UTR and miRNA plays an essential role in stabilizing the RNA duplex. The stability of the hydrogen bond network formed throughout the 20 ns MD simulation is depicted in Fig. 8C. From the plot it is evident that substantial number of hydrogen bonds are formed, and their pattern and number are found to be uniform throughout the simulation, and from this finding it can be deduced that RNA duplex remains stable throughout simulation and does not dissociate.

Radius of gyration (Rg) measures the compaction and extendedness of the complex of RNA duplex around the axis. The gradual increase in the Rg is an ideal indicator of duplex being dissociated, however in this case the Rg remains constant throughout the MD simulation with the values strictly falling between 2.08 and 2.09 nm, again highlighting the aspect of the stability of the RNA-RNA 3′UTR-miRNA duplex (Fig. 8 D). The Simulation video file of 3′UTR - csi-miR169–3p RNA duplex can be viewed in supplementary material named as Supplementary2_MD_Simulation.mp4.

4. Discussion

History of alternative medicine dates back to eighteenth century, where the incipient existence of present biomedicine paved way for practising an independent and complete medical system in certain parts of the world, leading to the development of Traditional Chinese medicine in Southeast part of Asia, Humoral theory in parts of Europe and the Ayurvedic medicine in the India subcontinent. The traditional medicines often used as spices and condiments in a regular Indian household have been used to treat various viral infections for a thousand of years in India. Some of the medicinal plants used in the Ayurvedic medicinal system more often are found to have immune system boosting ability [44]. Going by the "We are what we eat" philosophy, the most significant thing from an individual's perspective is to have a nutritious diet for a healthy living. A balanced diet with all vitamins, minerals, micro-nutrients, carbohydrates and other biomolecules would lead to build a strong immune system that can withstand the evolving viral attacks [11]. Furthermore, it is interesting to explore the cross-species links of how the pandemic caused by a virus is creating havoc for the mankind and how possibly the immunity provided by food.

miRNA-based antiviral methods are being developed as a consequence of research into the interaction between miRNAs and SARS-CoV-2. More than seven thousand COVID19 clinical trials have been registered and nearly two thousand such trials have been completed globally to date, ranging from convalescent plasma therapies, novel vaccine

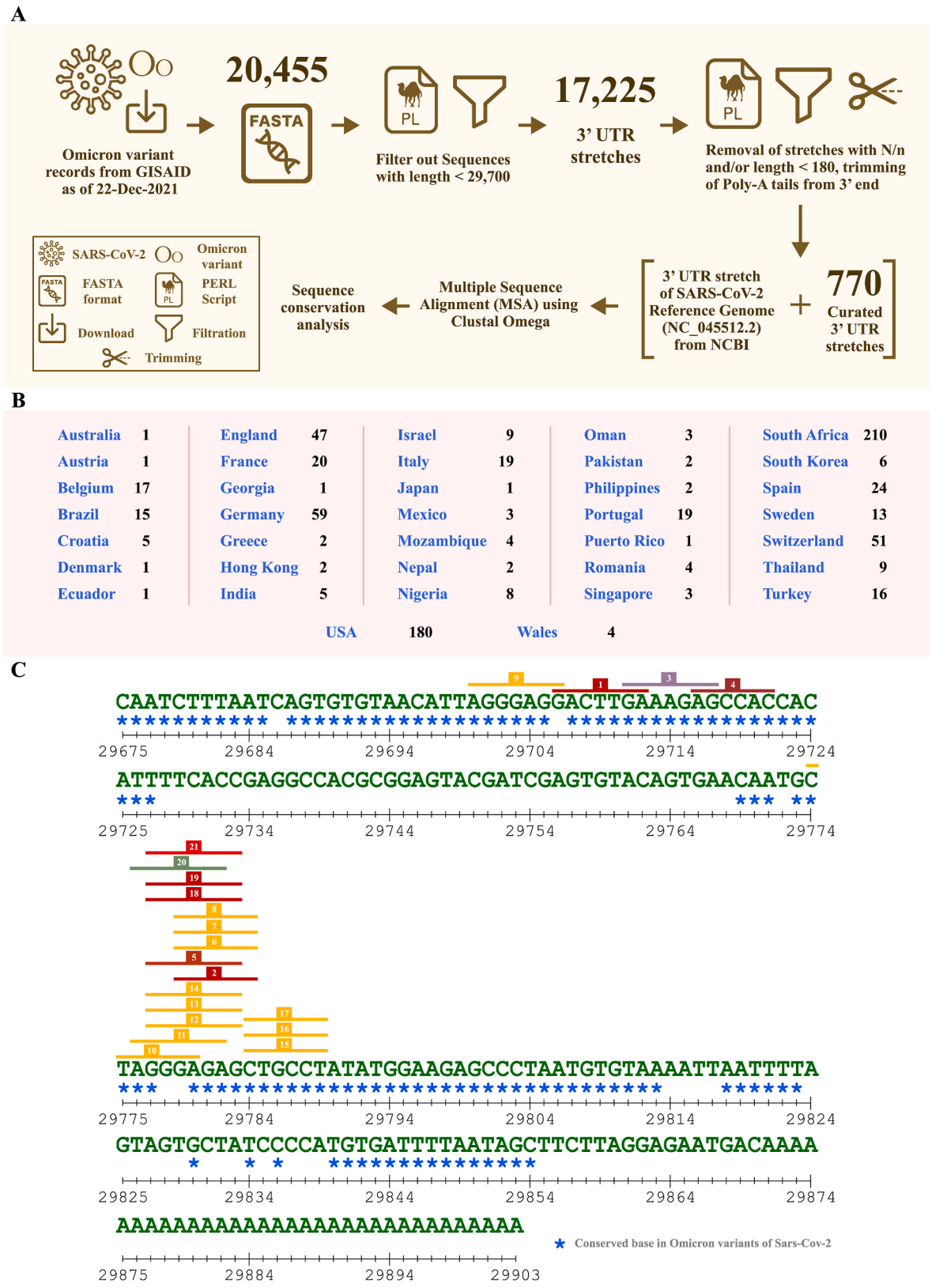

Fig. 6. A. Stepwise workflow starting from Omicron variant sequence collection from GISAID to the conservation analysis using Clustal Omega. **B.** Countries/territories across the globe and respective counts of the Omicron variant sequences. **C.** Base conservation in 3′UTR region of Omicron variant: The green alphabets represent the 3′UTR sequence of reference SARS-CoV-2 genome (NC_045512.2). Each "Blue asterisk" just below the reference base is showing the conservation of that base in 770 Omicron variants. The coloured horizontal bars with serial number represent the relative miRNAs and length of these bars reflects the aligned fruit miRNAs region with the 3′UTR of reference SARS-CoV-2 genome.

WHO Label	WHO Designation	Pango Lineage	Complete Genome Sequences	Curated Sequences	"CTGCCT" Site containing Curated Sequences (Percentage count out of total Curated Sequences)
ALPHA	VOC	B.1.1.7	194,915	36,402	36,332 (99.80%)
BETA	VOC	B.1.351	642	174	172 (98.85%)
GAMMA	VOC	P.1	6453	1592	1589 (99.81%)
DELTA	VOC	B.1.617.2	10,174	2840	2836 (99.85%)
LAMBDA	VOI	C.37	408	151	151 (100%)
MU	VOI	B.1.621	29	9	9 (100%)

VOC : Variant Of Concern VOI : Variant Of Interest

Fig. 7. Percentage and count of Conserved Site "CTGCCT" in other SARS-CoV-2 variants. The variant nomenclature is retrieved from WHO and Sequences were collected from NCBI.

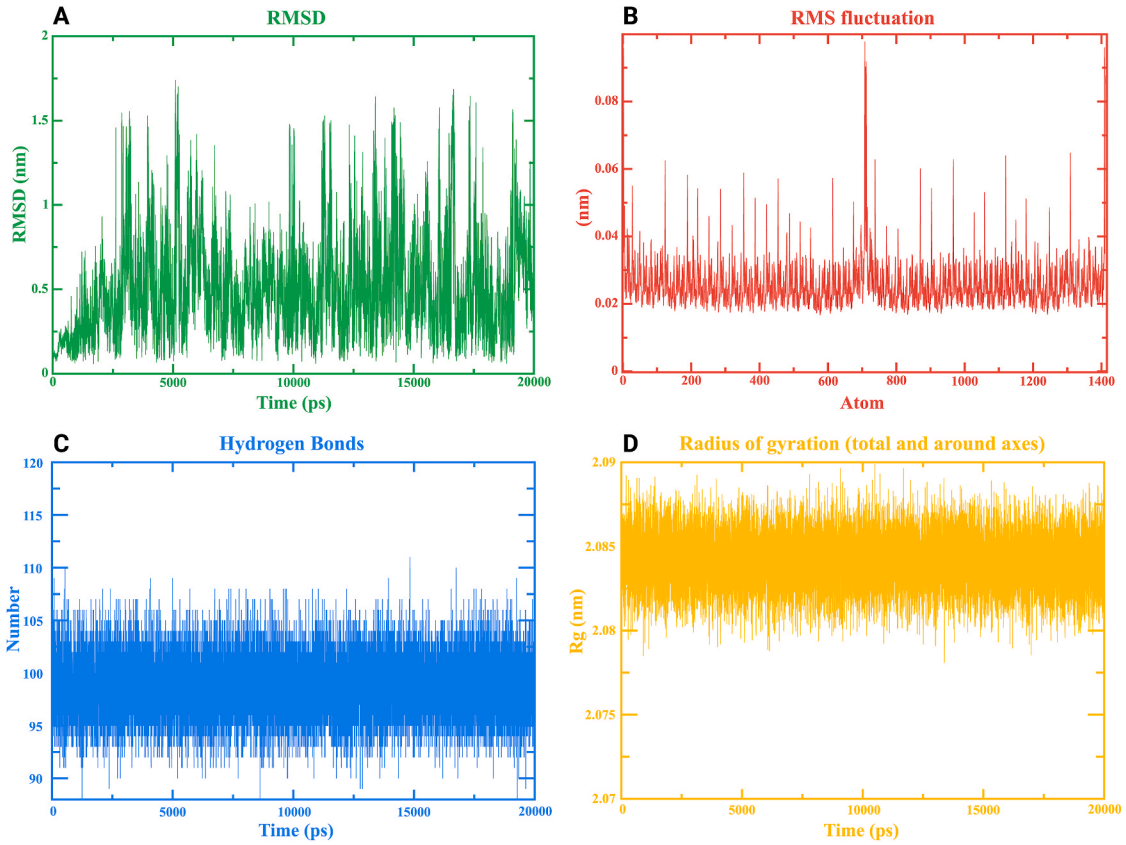

Fig. 8. Graphical representation of 20 ns Molecular Dynamic simulation for the 3′UTR-miR duplex A. Graphical representation of RMSD values B. RMSF fluctuation C. Hydrogen bond interaction D. Radius of gyration.

development to different drug repurposing strategies (such as Remdesivir and Favipiravir) [45]. Several COVID-19 vaccines have been approved for use by various regulatory agencies throughout the world and utilization of miRNA-based vaccines against SARS-CoV-2 have led to an expansion of miRNA-based research. Despite the development of successful vaccines, further research, particularly in light of new SARS-CoV-2 variations and potential vaccine-resistant strains, remains crucial [46].

Research work on cross-species interaction started off when the role of plant miRNA derived from *Oryza sativa*, namely miRNA168a was associated with modulating the molecular expression of Low-Density Lipoprotein Receptor Adaptor Protein 1 (LDLRAP1) and contributed to a better understanding of their role in plant-human interaction at the molecular level [14]. Besides, the efficiency of orally administered honeysuckle decoction was investigated after a study on mice with influenza strains and a clinical investigation on COVID-19 patients indicated that properly absorbed plant miRNA2911 had inhibitory effects against viral replication for the diseases [20,21]. According to recent review report, screening of conserved plant miRNAs against the hepatitis B (HBV) and C (HCV) viruses revealed six HCV gene sequences that are likely to be targeted by miR-156, miR-157, miR-166, miR-172, and miR-390. Whilst five conserved plant miRNAs: miR-166, miR-169, miR-172, miR-390, and miR-399 that were very likely to align and interact onto the six HBV gene sequences [19]. A report from our study group also revealed a cross-species interaction of plant miRNAs belonging to the family of miR477 ubiquitously found in all three medicinal plant genomes of *O. tenuiflorum*, *P. nigrum* and *Z. officinale* to pinpoint a plausible role of plant derived dietary miRNAs to mediate viral mRNA silencing and provide antiviral defence against SARS-CoV-2 infection [23]. These are all amongst the evidence which suggest the conjecture of the inhibitory role of exogenous miRNAs being inhibitory for SARS-CoV-2 viral replication.

This work was comprehended with the idea of identifying the conjecture of how consumption of fresh fruits, especially orange fruit on a regular basis can considerably act as a prophylactic in strengthening our immune system or probably as an anti-viral against not just SARS-COV-2 but also against its variant Omicron as identified by the WHO's Technical Advisory Group on Virus Evolution (TAG-VE) in November 2021 [6]. Plant miRNAs are the initial necessary material and hence mature miRNA sequences were retrieved from miRBase repository. miRBase is a data repository consisting of 48,860 mature and 38,589 pre-mature miRNA sequences of 271 organisms segregated into 6 main categories. For this particular study, the *Viridiplantae* eukaryotic clade was explored under the 'browse' tab and each plant mature miRNA sequences were retrieved manually with a count of 10,414 in FASTA format [25]. The reference genome sequence of SARS-CoV-2 was downloaded from NCBI. NCBI is a vast repository of online resources and biological information out of which, GenBank is an information and nucleic acid sequence retrieval system from where the first reported SARS-CoV-2 genome of Wuhan isolated was downloaded (NC_045512.2) in FASTA format [24,43]. The miRanda algorithm was used to find potential target sites for mature plant miRNAs in 3′UTR region of SARS-CoV-2 genomic sequence. According to the algorithm, local alignment [27] in complementary homology search was carried out between the query miRNA sequence and the reference genomic sequence and then approximates the thermodynamic stability of the highest scoring alignments by calculating the minimum free energy (kcal/mol) of the miRNA: 3′UTR duplex [28]. The primary 220 hits on the viral 3′UTR were filtered based on: i) minimum energy of $\Delta G \leq -14$ kcal/mol of the miRNA: 3′UTR duplex and ii) hybridization alignment score $\geq$80 [26] resulted in 148 hits. Further the gene-regulatory target site recognition was done by following rules proposed in literature [29] to identify the final 111 hits followed by the 21 edible fruit derived hits. The Omicron variant sequences of SARS-CoV-2 were downloaded from GISAID. GISAID is a comprehensive initiative of data science and fundamental origin of genomic and related metadata resource of influenza virus, Respiratory Syncytial Virus, and SARS-CoV-2 [30]. A Total of 20,455 Omicron variant records (as of Dec-22-2021) in FASTA format were retrieved from GISAID followed by filtration step (length>29,700) generated 17,225 sequences, which were processed to capture 3′UTR region and further filtration (3′UTR capture, length>180, no N/n) resulted in 770 curated Omicron 3′UTR fragments from 37 countries/territories worldwide. Multiple Sequence Alignment (MSA) was performed using Clustal Omega to confirm the applicability of the 21 fruit miRNAs on Omicron variant. Clustal Omega program can effectively perform MSA on even larger datasets with fast result delivery without compromising the accuracy [31]. Hence, the 770 curated 3′UTR stretches of Omicron variants along with the 3′UTR of reference SARS-CoV-2 genome (NC_045512.2) were processed using Clustal Omega to get the base conservation information.

There were few major observations of the base conservation analysis amongst the 3′UTR region of reference genome SARS-CoV-2 and other variants. Firstly, it was observed that the Omicron variant still holds into account about 117 bases to be conserved out of a total of 196 bases long 3′UTR region of reference SARS-CoV-2 genome excluding Poly-A tail residues. The conserved region is divided in two clusters which is mainly divided amongst 5 long stretches: i) 29675–29685 (11 bases) ii) 29687–29705 (19 bases) iii) 29707–29727 (21 bases) iv) 29780–29813 (34 bases) and v) 29840–29854 (15 bases). Secondly, as we performed the alignment of 3′UTR for Omicron strains with the filtered 21 'raw-eatable' fruit miRNAs using miRanda algorithm, we identified that the major portion of these 21 miRNAs is covered by miR-477 family on the 3′UTR region. The 2 miRNAs namely vvi-miR477b-5p and ssp-miR444b.1 were found to be having conserved target regions at a stretch of "GAAAGAG" (29711–29717) and "AGCCAC" (29716–29721) respectively. Additionally, another observation from the miRanda algorithm analysis was that 17 of 21 'raw-eatable' plant miRNAs were targeting the 16-base region (29774–29789) which is almost a conserved region except the 2 residues. In this 16-base region, we identified a 6-base region "CTGCCT", found to be fully conserved amongst the reference genome and all 770 Omicron variant genomes 3′UTR, which is targeted by particularly 3 miRNAs belonging to the species *Citrus sinensis* namely, csi-miR169c-3p, csi-miR169d-3p and csi-miR169e-3p. This same "CTGCCT" site was also searched not only in the Omicron sequences but also amongst other variants of SARS-CoV-2. The energy values for all these three *Citrus sinensis* miRNAs against that of SARS-CoV-2 and its variant 3′UTR region was found to be of the lowest of −26.68 kcal/mol (Fig. 5 A) displaying the higher thermodynamic stability and thus providing the first evidence of dietary plant miRNA of miR169–3p family derived from *Citrus sinensis* (Orange) to target the viral 3′UTR region. Additionally, to ensure the thermodynamic robustness of the RNA duplex of 3′UTR and *Citrus sinensis* csi-miR169c-3p, we undertook MD simulation of the duplex for a period of 20 ns. Assessment based on the values of RMSF, RMSD, hydrogen bond interaction and Radius of gyration highlight the overall stability of the nucleotide complex for majority period of the simulation. Furthermore, the conserved site "CTGCCT" comprises a higher percentage of GC content, also seen through the simulation profile and thereby holds a substantial impact on producing a stable interaction with csi-miR169–3p to become a promising target sequence.

5. Conclusion

With the belief that nutrients from fruits are known to possess strong immunomodulatory actions to uphold the defence against viral infection, thereby minimising the disease progression and severity along with the likeliness of being prophylactic. We here highlight the importance of dietary plant miRNAs found in fruits like *Citrus sinensis* (Orange), *Prunus persica* (Peaches), *Vitis vinifera* (Grapes), *Malus domestica* (Apple) amongst other to include in our daily diet. Especially the strong interaction between *Citrus sinensis* (Orange) miRNA cluster of miR169–3p family and the conserved site "CTGCCT" present in reference SARS-CoV-2 genome and all 770 curated Omicron variants from 37 regions worldwide. In continuation this site is also conserved in other variants of SARS-CoV-2 hence the consumption of especially orange may help the infected patients globally. This understanding of raw edible plant-virus cross kingdom interaction opens the door to the possibility that fruit miRNAs, like vitamins and minerals, may serve as a dietary component and imitate the actions of our indigenous miRNAs in regulating molecular activity under ill health and hence proposing the daily consumption of orange. This study not only testifies to the function of dietary plant miRNAs in strengthening human defence against viruses, but also reveals a conserved region in the SARS-CoV-2 genome that might be a good research target for tackling the perils of COVID-19.

Funding

The computational analysis in this study was supported by Bioinformatics Node facility provided by Gujarat State Biotechnology Mission (GSBTM), Department of Science & Technology (DST) and Government of Gujarat [Grant number: GSBTM/MD/JDR/1409/2017–18].

Role of the funding source

The funding sponsors had no role in the study design, in the collection, analysis and interpretation of data; in the writing of the manuscript; and in the decision to submit the manuscript for publication.

Availability of data and material

The additional data is provided in Supplementary material.

Code availability

Not applicable.

CRediT authorship contribution statement

Naman Mangukia: Conceptualization, Methodology, Formal analysis, Data curation, Writing - Original Draft, Writing - review and editing. **Priyashi Rao:** Molecular dynamic Simulation methodology and analysis, Writing - Original Draft, Writing - review and editing. **Kamlesh Patel:** Supervision. **Himanshu Pandya:** Supervision. **Rakesh M. Rawal:** Conceptualization, Supervision.

Authors approval

All authors have read and approved the final manuscript.

Ethics approval

The manuscript does not contain experiments using animals and does not contain human studies.

Declaration of competing interest

All authors declare no conflict of interest.

Acknowledgement

Authors would like to acknowledge the worldwide community of researchers for sharing the complete genome data of SARS-CoV-2 and its variants at NCBI and GISAID (Supplementary1_NCBI_and_GISAID_Acknowledgement.xlsx). Authors thank the invaluable inputs of Mr. Parth Gosai in Graphic designing. Authors thank Ms. Sukanya Raval for proofreading the manuscript. Author Naman Mangukia acknowledges the Prime Minister's Fellowship (PMF) award from Science and Engineering Research Board (SERB), Department of Science and technology (DST), Government of India, Confederation of Indian Industry (CII) and industry support aided by BioInnovations. Author Priyashi Rao would like to extend gratitude to the ScHeme Of Developing High quality research (SHODH), Education department, Government of Gujarat, India for providing the student support fellowship.

Appendix A. Supplementary data

Supplementary data to this article can be found online at https://doi.org/10.1016/j.compbiomed.2022.105502.

References

[1] L. Spinney, How pandemics shape social evolution, Nature 574 (2019) 324–326, https://doi.org/10.1038/d41586-019-03048-8.
[2] D. Cucinotta, M. Vanelli, WHO declares COVID-19 a pandemic, Acta Biomed. 91 (2020) 157–160, https://doi.org/10.23750/ABM.V91I1.9397.
[3] World Health Organization, Coronavirus disease (COVID-19) situation reports in Bnagladesh, World Heal. Organ. 75 (2020) 1. https://www.who.int/emergencies/diseases/novel-coronavirus-2019/situation-reports/. (Accessed 15 October 2020).
[4] Centre for Disease Prevention and Control (CDC), Symptoms of COVID-19 | CDC, CDC (2021). https://www.cdc.gov/coronavirus/2019-ncov/symptoms-testing/symptoms.html. (Accessed 28 December 2021).
[5] J. Prajapati, P. Rao, L. Poojara, D. Goswami, D. Acharya, S.K. Patel, R.M. Rawal, Unravelling the antifungal mode of action of curcumin by potential inhibition of CYP51B: a computational study validated in vitro on mucormycosis agent, Rhizopus oryzae, Arch. Biochem. Biophys. 712 (2021) 109048, https://doi.org/10.1016/j.abb.2021.109048.
[6] World Health Organization, Tracking SARS-CoV-2 variants, Who (2021). https://www.who.int/en/activities/tracking-SARS-Co. (Accessed 27 December 2021). https://www.who.int/en/activities/tracking-SARS-CoV-2-variants/.
[7] J. Chen, R. Wang, N.B. Gilby, G.-W. Wei, Omicron (B.1.1.529): infectivity, vaccine breakthrough, and antibody resistance, ArXiv. (2021)./pmc/articles/PMC8647651/(accessed December 27, 2021).
[8] E. Callaway, Heavily mutated Omicron variant puts scientists on alert, Nature 600 (2021) 21, https://doi.org/10.1038/d41586-021-03552-w, 21.
[9] F. Aman, S. Masood, How Nutrition can help to fight against COVID-19 Pandemic, Pakistan J. Med. Sci. 36 (2020) S121, https://doi.org/10.12669/PJMS.36.COVID19-S4.2776.
[10] S. Farhadi, R.S. Ovchinnikov, The relationship between nutrition and infectious diseases: a review, Biomed. Biotechnol. Res. J. 2 (2018) 168, https://doi.org/10.4103/BBRJ.BBRJ_69_18.
[11] P.C. Calder, A.C. Carr, A.F. Gombart, M. Eggersdorfer, Optimal nutritional status for a well-functioning immune system is an important factor to protect against viral infections, Nutrients 12 (2020), https://doi.org/10.3390/nu12041181.
[12] J. O'Brien, H. Hayder, Y. Zayed, C. Peng, Overview of microRNA biogenesis, mechanisms of actions, and circulation, Front. Endocrinol. 9 (2018) 402, https://doi.org/10.3389/fendo.2018.00402.
[13] E. Girardi, P. López, S. Pfeffer, On the importance of host MicroRNAs during viral infection, Front. Genet. 9 (2018), https://doi.org/10.3389/fgene.2018.00439.
[14] L. Zhang, D. Hou, X. Chen, D. Li, L. Zhu, Y. Zhang, J. Li, Z. Bian, X. Liang, X. Cai, Y. Yin, C. Wang, T. Zhang, D. Zhu, D. Zhang, J. Xu, Q. Chen, Y. Ba, J. Liu, Q. Wang, J. Chen, J. Wang, M. Wang, Q. Zhang, J. Zhang, K. Zen, C.Y. Zhang, Exogenous plant MIR168a specifically targets mammalian LDLRAP1: evidence of cross-kingdom regulation by microRNA, Cell Res. 22 (2012) 107–126, https://doi.org/10.1038/cr.2011.158.
[15] D. Hou, F. He, L. Ma, M. Cao, Z. Zhou, Z. Wei, Y. Xue, ScienceDirect the potential atheroprotective role of plant MIR156a as a repressor of monocyte recruitment on inflamed human endothelial cells, J. Nutr. Biochem. 57 (2018) 197–205, https://doi.org/10.1016/j.jnutbio.2018.03.026.
[16] X. Wang, X. Ren, L. Ning, P. Wang, K. Xu, Stability and absorption mechanism of typical plant miRNAs in an in vitro gastrointestinal environment: basis for their cross-kingdom nutritional effects, J. Nutr. Biochem. 81 (2020), https://doi.org/10.1016/j.jnutbio.2020.108376.
[17] J. Link, C. Thon, D. Schanze, R. Steponaitiene, J. Kupcinskas, M. Zenker, A. Canbay, P. Malfertheiner, A. Link, Food-derived xeno-microRNAs : influence of diet and detectability in gastrointestinal tract, Proof-of-Principle Study 1800076 (2019) 1–11, https://doi.org/10.1002/mnfr.201800076.
[18] Q. Chen, F. Zhang, L. Dong, H. Wu, J. Xu, H. Li, J. Wang, Z. Zhou, C. Liu, Y. Wang, Y. Liu, L. Lu, C. Wang, M. Liu, X. Chen, C. Wang, C. Zhang, D. Li, K. Zen, F. Wang, Q. Zhang, C.Y. Zhang, SIDT1-dependent absorption in the stomach mediates host uptake of dietary and orally administered microRNAs, Cell Res. 31 (2021) 247–258, https://doi.org/10.1038/s41422-020-0389-3.
[19] D. Li, J. Yang, Y. Yang, J. Liu, H. Li, R. Li, C. Cao, L. Shi, W. Wu, K. He, A timely review of cross-kingdom regulation of plant-derived MicroRNAs, Front. Genet. 12 (2021) 702, https://doi.org/10.3389/FGENE.2021.613197/BIBTEX.
[20] Z. Zhou, X. Li, J. Liu, L. Dong, Q. Chen, J. Liu, H. Kong, Q. Zhang, X. Qi, D. Hou, L. Zhang, G. Zhang, Y. Liu, Y. Zhang, J. Li, J. Wang, X. Chen, H. Wang, J. Zhang, H. Chen, K. Zen, C.Y. Zhang, Honeysuckle-encoded atypical microRNA2911 directly targets influenza A viruses, Cell Res. 25 (2015) 39–49, https://doi.org/10.1038/cr.2014.130.
[21] L.K. Zhou, Z. Zhou, X.M. Jiang, Y. Zheng, X. Chen, Z. Fu, G. Xiao, C.Y. Zhang, L. K. Zhang, Y. Yi, Absorbed plant MIR2911 in honeysuckle decoction inhibits SARS-CoV-2 replication and accelerates the negative conversion of infected patients, Cell Discov 6 (2020) 4–7, https://doi.org/10.1038/s41421-020-00197-3.
[22] D. Cavalieri, L. Rizzetto, N. Tocci, D. Rivero, E. Asquini, A. Si-Ammour, E. Bonechi, C. Ballerini, R. Viola, Plant microRNAs as novel immunomodulatory agents, Sci. Rep. 6 (2016), https://doi.org/10.1038/srep25761.
[23] N. Mangukia, P. Rao, K. Patel, H. Pandya, R.M. Rawal, Identifying potential human and medicinal plant microRNAs against SARS-CoV-2 3′UTR region: a computational genomics assessment, Comput, Biol. Med. 136 (2021), https://doi.org/10.1016/j.compbiomed.2021.104662.
[24] E.W. Sayers, J. Beck, E.E. Bolton, D. Bourexis, J.R. Brister, K. Canese, D.C. Comeau, K. Funk, S. Kim, W. Klimke, A. Marchler-Bauer, M. Landrum, S. Lathrop, Z. Lu, T. L. Madden, N. O'Leary, L. Phan, S.H. Rangwala, V.A. Schneider, Y. Skripchenko, J. Wang, J. Ye, B.W. Trawick, K.D. Pruitt, S.T. Sherry, Database resources of the national center for Biotechnology information, Nucleic Acids Res. 49 (2021) D10–D17, https://doi.org/10.1093/nar/gkaa892.
[25] A. Kozomara, M. Birgaoanu, S. Griffiths-Jones, MiRBase: from microRNA sequences to function, Nucleic Acids Res. 47 (2019) D155–D162, https://doi.org/10.1093/nar/gky1141.
[26] A.J. Enright, B. John, U. Gaul, T. Tuschl, C. Sander, D.S. Marks, MicroRNA targets in Drosophila, Genome Biol. 5 (2003) 1–14, https://doi.org/10.1186/gb-2003-5-1-r1.
[27] T.F. Smith, M.S. Waterman, Identification of common molecular subsequences, J. Mol. Biol. 147 (1981) 195–197, https://doi.org/10.1016/0022-2836(81)90087-5.
[28] S. Wuchty, W. Fontana, I.L. Hofacker, P. Schuster, Complete suboptimal folding of RNA and the stability of secondary structures, Biopolymers 49 (1999) 145–165, https://doi.org/10.1002/(SICI)1097-0282(199902)49:2<145::AID-BIP4>3.0.CO;2-G.
[29] D.P. Bartel, MicroRNAs: target recognition and regulatory functions, Cell 136 (2009) 215–233, https://doi.org/10.1016/j.cell.2009.01.002.
[30] Y. Shu, J. McCauley, GISAID: global initiative on sharing all influenza data – from vision to reality, Euro Surveill. 22 (2017) 2–4, https://doi.org/10.2807/1560-7917.ES.2017.22.13.30494.
[31] F. Sievers, A. Wilm, D. Dineen, T.J. Gibson, K. Karplus, W. Li, R. Lopez, H. McWilliam, M. Remmert, J. Söding, J.D. Thompson, D.G. Higgins, Fast, scalable generation of high-quality protein multiple sequence alignments using Clustal Omega, Mol. Syst. Biol. 7 (2011), https://doi.org/10.1038/msb.2011.75.

[32] I.L. Hofacker, Vienna RNA secondary structure server, Nucleic Acids Res. 31 (2003) 3429–3431, https://doi.org/10.1093/nar/gkg599.
[33] M. Popenda, M. Szachniuk, M. Antczak, K.J. Purzycka, P. Lukasiak, N. Bartol, J. Blazewicz, R.W. Adamiak, Automated 3D structure composition for large RNAs, Nucleic Acids Res. 40 (2012), https://doi.org/10.1093/NAR/GKS339.
[34] M. Antczak, M. Popenda, T. Zok, J. Sarzynska, T. Ratajczak, K. Tomczyk, R. W. Adamiak, M. Szachniuk, New functionality of RNAComposer: an application to shape the axis of miR160 precursor structure, Acta Biochim. Pol. 63 (2016) 737–744, https://doi.org/10.18388/ABP.2016_1329.
[35] E.F. Pettersen, T.D. Goddard, C.C. Huang, G.S. Couch, D.M. Greenblatt, E.C. Meng, T.E. Ferrin, UCSF Chimera—a visualization system for exploratory research and analysis, J J. Comput. Chem. 25 (2004) 1605–1612.
[36] H. Bekker, H.J.C. Berendsen, E.W. Dijkstra, S. Achterop, R. van Drunen, D. der Spoel, H. Bekker, E.J. Dijkstra, D. Van Der Spoel, A. Sijbers, Gromacs: A Parallel Computer for Molecular Dynamics Simulations, 1993.
[37] D. Van Der Spoel, E. Lindahl, B. Hess, G. Groenhof, A.E. Mark, H.J.C. %J J. Of Computational Chemistry Berendsen, GROMACS: Fast, Flexible, and Free, 26, 2005, pp. 1701–1718.
[38] S. Pronk, S. Páll, R. Schulz, P. Larsson, P. Bjelkmar, R. Apostolov, M.R. Shirts, J. C. Smith, P.M. Kasson, D. Van Der Spoel, B. Hess, E. Lindahl, Gromacs 4.5: a high-throughput and highly parallel open source molecular simulation toolkit, Bioinformatics 29 (2013) 845–854, https://doi.org/10.1093/bioinformatics/btt055.
[39] B. Hess, H. Bekker, H.J.C. Berendsen, J.G.E.M. %J J. Of Computational Chemistry Fraaije, LINCS: a Linear Constraint Solver for Molecular Simulations, 18, 1997, pp. 1463–1472.
[40] P.J. %J C. For C. Turner, O.G.I. of S. Land-Margin Research, B. Technology OR, XMGRACE, Version 5.1. 19, 2005.
[41] C. Cao, Z. Cai, X. Xiao, J. Rao, J. Chen, N. Hu, M. Yang, X. Xing, Y. Wang, M. Li, B. Zhou, X. Wang, J. Wang, Y. Xue, The architecture of the SARS-CoV-2 RNA genome inside virion, Nat. Commun. 12 (2021) 1–14, https://doi.org/10.1038/s41467-021-22785-x.
[42] L.D. Rizkita, I. Astuti, The potential of miRNA-based therapeutics in severe acute respiratory syndrome coronavirus 2 (SARS-CoV-2) infection: a review, J. Pharm. Anal. 11 (2021) 265, https://doi.org/10.1016/J.JPHA.2021.03.003.
[43] F. Wu, S. Zhao, B. Yu, Y. Chen, W. Wang, Z. Song, Y. Hu, Z. Tao, J. Tian, Y. Pei, M. Yuan, Y. Zhang, F. Dai, Y. Liu, Q. Wang, J. Zheng, L. Xu, E. Holmes, Y. Zhang, A new coronavirus associated with human respiratory disease in China. https://doi.org/10.1038/s41586-020-2202-3, 2020, 580, E7.
[44] S. Borse, M. Joshi, A. Saggam, V. Bhat, S. Walia, A. Marathe, S. Sagar, P. Chavan-Gautam, A. Girme, L. Hingorani, G. Tillu, Ayurveda botanicals in COVID-19 management: an in silico multi-target approach, PLoS One 16 (2021), https://doi.org/10.1371/JOURNAL.PONE.0248479.
[45] D.H.P. Damasceno, A.A. Amaral, C.A. Silva, A.C. Simões e Silva, The impact of vaccination worldwide on SARS-CoV-2 infection: a review on vaccine mechanisms, results of clinical trials, vaccinal coverage and interactions with novel variants, Curr. Med. Chem. 28 (2021), https://doi.org/10.2174/0929867328666210902094254.
[46] C. Hum, J. Loiselle, N. Ahmed, T.A. Shaw, C. Toudic, J.P. Pezacki, MicroRNA mimics or inhibitors as antiviral therapeutic approaches against COVID-19, Drugs 81 (2021) 517–531, https://doi.org/10.1007/s40265-021-01474-5.